Check for updates

Improving the energy yield of plasma-based NO$_x$ synthesis with *in situ* adsorption†

Kevin Hendrik Reindert Rouwenhorst, [iD] [abc] Sybe Tabak[a] and Leon Lefferts [iD] *[a]

Plasma-based NO$_x$ synthesis from air is a promising option to electrify nitrogen fixation. However, the energy efficiency of direct plasma-based NO$_x$ synthesis in a plasma reactor is severely limited by NO$_x$ decomposition in the plasma phase. *In situ* NO$_x$ adsorption on MgO improves the NO$_x$ energy yield in a dielectric barrier discharge (DBD) plasma reactor by a factor of 15.

Plasma-based nitrogen fixation *via* NO$_x$ synthesis from air was commercialized in the early 20th century. Kristian Birkeland and Samuel Eyde commercialized the first industrial nitrogen fixation process, the Birkeland–Eyde process, based on an electric arc plasma reactor.[1,2] This process was operational in Norway and Canada.[3,4] However, the process was eventually outcompeted by the Haber–Bosch process, producing ammonia (NH$_3$) from nitrogen (N$_2$) and hydrogen (H$_2$) derived from steam reforming of hydrocarbons or from water electrolysis.

Plasma-based nitrogen fixation has re-emerged in scientific literature as an option to electrify N$_2$ fixation.[5–9] Plasma-based processes have the advantage that the load can be varied quickly, in contrast to thermal processes, so that rapid changes in supply of renewable electricity can be handled.[10] Also, absence of the need for intensive energy integration makes local production at relatively small scale feasible. In particular, plasma-N$_2$ fixation in the form of NO$_x$ shows promise.[5,6]

[a] *Catalytic Processes & Materials, MESA+ Institute for Nanotechnology, University of Twente, P.O. Box 217, 7500 AE Enschede, The Netherlands.*
E-mail: l.lefferts@utwente.nl
[b] *Ammonia Energy Association, 77 Sands Street, 6th Floor, Brooklyn, NY 11201, USA*
[c] *Koolen Industries, Europalaan 202, 7559 SC Hengelo, The Netherlands*

So far, plasma-based NO$_x$ synthesis in warm plasma reactors such as gliding arc (GA) and microwave (MW) plasma reactors, shows the best performance,[5,6] with NO$_x$ formation at an energy cost down to 0.42 MJ per mol NO$_x$,[11] which is competitive with the renewable Haber–Bosch process (using electrolysis to produce H$_2$) combined with the Ostwald process (NH$_3$ oxidation) in terms of energy cost (0.6 MJ per mol HNO$_3$).[6] However, such low energy consumptions for plasma reactors are only achieved when operating at low NO$_x$ concentrations of typically a few hundred ppm,[11] which is not practical for NO$_x$ absorption in water in an industrial process.[12] Concentrations in the order of 5 mol% NO$_x$ are required for efficient processing. For those conditions, the energy consumption for NO$_x$ formation in plasma reactors is at least in the order of 2 MJ per mol NO$_x$.[6] Furthermore, the high temperatures in warm plasmas in the order of 10^3 K cause thermal NO$_x$ decomposition[13] and rapid quenching is required to minimize thermal NO$_x$ decomposition.

This work introduces a novel concept for energy-efficient NO$_x$ formation in a dielectric barrier discharge (DBD) reactor *via in situ* NO$_x$ removal using a solid MgO sorbent. A DBD reactor is a non-thermal plasma reactor operating near room temperature.[14] Only a few studies have been done using DBD reactors for NO$_x$ synthesis,[13,15–18] reporting relatively high energy consumption compared to warm plasma reactors. Nevertheless, a DBD reactor has been used in this work for two reasons. Firstly, thermal NO$_x$ decomposition is negligible at mild temperature, and secondly, *in situ* NO$_x$ removal *via* adsorption on a solid sorbent is easily achievable. Product molecules adsorbed on microporous materials are protected against plasma induced decomposition in a DBD reactor, as we have demonstrated earlier for the case of ammonia synthesis in a DBD reactor.[19] Plasma cannot develop in sub-micron pores while plasma activated species are too short-lived to diffuse into these pores; therefore adsorbed molecules are protected against plasma-decomposition.[8] Suppressing NO$_x$ decomposition is expected to improve both energy efficiency and the single pass conversion in a DBD

528 | *React. Chem. Eng.*, 2024, **9**, 528–531

This journal is © The Royal Society of Chemistry 2024

reactor. As earth-alkali metal oxides are known to sorb NO_x,[20] we have selected MgO to demonstrate this concept. We will show that both energy efficiency as well as NO_x concentrations in the product stream are drastically improved.

High surface area MgO (294 m² g⁻¹) with a particle size between 250 and 300 μm was prepared and characterized as described in ESI† section S1. The experiments were performed using a packed bed DBD reactor with MgO particles, and the NO_x concentration was determined with a mass spectrometer (MS), as described in detail in section S2.1.†

Fig. 1 shows the NO_x concentration in the outlet as a function of time on igniting the plasma, operating with an O_2 : N_2 ratio of 1 : 1, flow rate of 20 mL min⁻¹, plasma power of 6.4 W, implying a SEI (specific energy input) of 19.2 kJ L⁻¹. The corresponding Lissajous plot is shown in Fig. S3 (see ESI†). It is observed that the NO_x outlet concentration is about 0.1 mol% during the first 4 min and increases to about 0.5 mol% afterwards. The change in NO_x outlet concentration with time in Fig. 1 is attributed to adsorption of NO_x on the MgO sorbent, followed by breakthrough of the NO_x in the outlet.

The result shown in Fig. 2 confirms that NO_x is indeed adsorbed *in situ*. After exposure to the plasma, the reactor was heated (25 °C min⁻¹) in N_2 (10 mL min⁻¹), inducing desorption of NO_x in absence of plasma. The concentration of NO_2 is much higher than NO, but we cannot rule out NO formation, as explained in ESI 3.3.† The NO_x concentration during desorption is up to 4%, one order of magnitude higher than the NO_x concentration during steady-state plasma operation. The amount adsorbed NO_x is 0.05 mol per mol MgO.

Fig. 3 compares the TPD (temperature programmed desorption) result after NO_x synthesis by plasma illumination during different times with TPD after adsorption of NO_2 at room temperature. The amount of NO_x formed during the plasma experiment obviously varies with plasma time. Fig. 4 shows that the amount of NO_x detected with TPD is already

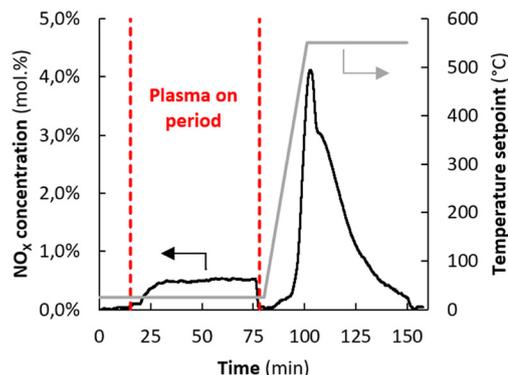Fig. 2 Typical result of plasma-based NO_x synthesis with *in situ* adsorption. Reactor temperature (left axis) and outlet NO_x MS signal (right axis) as a function of time. Oven temperature set point during plasma, 25 °C; total flow rate, 20 mL min⁻¹; O_2 : N_2 = 1 : 1; plasma power, 6.4 W (SEI = 19.2 kJ L⁻¹); MgO loading, 300 mg (250–300 μm); plasma duration, 63 min; heating rate after plasma-based NO_x synthesis, 25 °C min⁻¹; pure N_2, 10 mL min⁻¹. Samples are thermally pre-treated at 550 °C in N_2.

saturated after typically 5 minutes of plasma exposure. The amount is slightly lower than after thermal NO_2 adsorption in absence of plasma (0.055 mol-NO_2 per mol-MgO), in the same order of magnitude as reported by Duong *et al.*[21] for MgO with a slightly lower surface area of 126 m² g⁻¹. The lower amount observed during NO_x synthesis with plasma is likely attributed to mild heating induced by the plasma, causing weakly adsorbed NO_2 to desorb. A similar effect was previously reported for *in situ* NH_3 removal by a zeolite for plasma-based NH_3 synthesis.[19] The effective NH_3 capacity on zeolite 4A decreased by 60% due to heating effects.[19]

The significance of the *in situ* adsorption of NO_x from the plasma zone is evident from the reduction in energy consumption *versus* steady-state operation. Steady-state NO_x synthesis in this work results in an energy consumption of 93 MJ per mol NO_x, in line with literature values reported in the
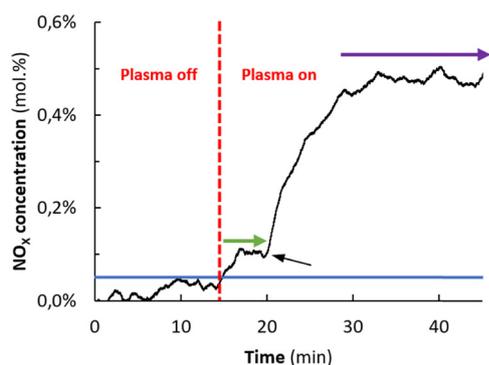

Fig. 1 Outlet NO_x concentration as a function of the plasma duration. Oven temperature set point, 25 °C; total flow rate, 20 mL min⁻¹; O_2 : N_2 = 1 : 1; plasma power, 6.4 W (SEI = 19.2 kJ L⁻¹); MgO loading, 300 mg (250–300 μm). The blue line represents the MS sensitivity limit. The green arrow line indicates *in situ* NO_x removal with MgO. The black arrow indicates breakthrough of NO_x due to sorbent saturation. The purple arrow indicates steady-state operation.
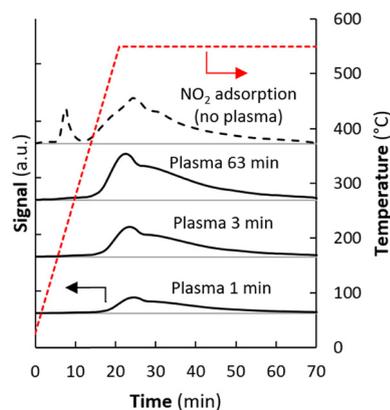

Fig. 3 TPD curve results after plasma-based NO_x synthesis (O_2 : N_2 = 1 : 1, plasma duration varied: 1 min, 3 min & 63 min), flow rate 20 mL min⁻¹ compared to TPD curve after adsorption of NO_2 at room temperature (2 vol% NO_2 in 10 vol% O_2 and 88 vol% N_2 balance gas during adsorption). TPD in pure N_2, 10 mL min⁻¹ and heating rate 25 °C min⁻¹.
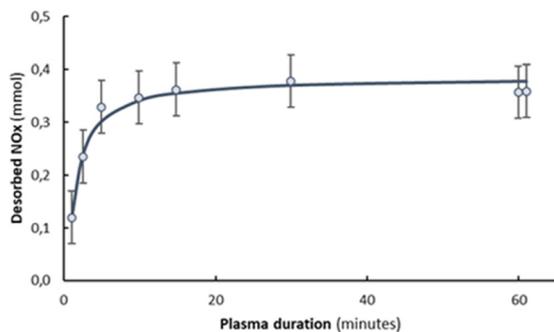
Fig. 4 The effect of plasma duration for plasma-based NO$_x$ synthesis with *in situ* adsorption on the amount of adsorbed NO$_x$ on 300 mg MgO.
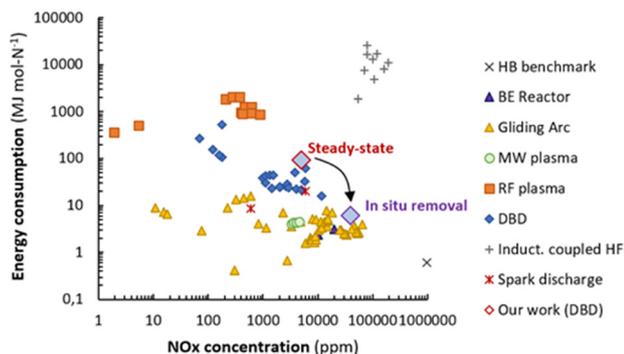

Fig. 5 Comparison of energy consumption for NO$_x$ production in various plasma reactors. Original figure reproduced from ref. 6, and data from this work added. Steady-state: red lined diamond. *In situ* removal: purple lined diamond.

range 16–540 MJ per mol NO$_x$ for DBD reactors.[13,15–18] In case of *in situ* product removal during 5 minutes, the energy consumption for the plasma reactor and NO$_x$ product desorption decreases to 6.0 MJ per mol NO$_x$ as calculated in section S3.2† including the energy cost of the desorption step. Effectively, the energy consumption efficiency is improved by a factor 15. As shown in Fig. 5, *in situ* adsorption of NO$_x$ in a DBD reactor results in the best performance for a non-thermal plasma-reactor, by both decreasing the energy consumption as well as increasing the NO$_x$ concentration in the product stream. Importantly, the NO$_x$ concentration raised well above 1%, which is considered as the minimum concentration required for nitric acid production by adsorption in water in a commercially viable process.[22]

Concluding, this work demonstrates that low temperature DBD plasma reactors can produce NO$_x$ with similar low energy consumptions obtained with warm plasma reactors like gliding arc reactors and microwave reactors (Fig. 5), by integrating plasma conversion and product separation. Also, the NO$_x$ concentration in the product stream is significantly increased. This study demonstrates the concept, but optimization of the (earth-)alkali material as well of the morphology of the adsorbent is likely to result in further improvement.[20] Furthermore, addition of a catalyst,[23] optimization of the dielectric

properties of the adsorbent,[18] and optimization of the plasma properties could be considered.[24,25]

In situ product removal is relevant for the wider scientific community working on plasma(-catalytic) conversion. We demonstrate that a significant improvement for NO$_x$ synthesis and it is likely that the concept would also applicable for plasma-based CO$_2$ dissociation and CH$_4$ conversion.[26]

Conflicts of interest

There are no conflicts to declare.

Acknowledgements

Notes and references

1 K. Birkeland, *Trans. Faraday Soc.*, 1906, **2**, 98–116.
2 S. Eyde, *J. Ind. Eng. Chem.*, 1912, **4**, 771–774.
3 A. S. Travis, *Nitrogen Capture: The Growth of an International Industry (1900–1940)*, Springer International Publishing, 2018.
4 K. H. R. Rouwenhorst, A. S. Travis and L. Lefferts, *Sustainable Chem.*, 2022, **3**, 149–171.
5 B. S. Patil, Q. Wang, V. Hessel and J. Lang, *Catal. Today*, 2015, **256**, 49–66.
6 K. H. R. Rouwenhorst, F. Jardali, A. Bogaerts and L. Lefferts, *Energy Environ. Sci.*, 2021, **14**, 2520–2534.
7 N. Cherkasov, A. O. Ibhadon and P. Fitzpatrick, *Chem. Eng. Process.*, 2015, **90**, 24–33.
8 A. Bogaerts, X. Tu, J. C. Whitehead, G. Centi, L. Lefferts, O. Guaitella, F. Azolina-Jury, H.-H. Kim, A. B. Murphy, W. F. Schneider, T. Nozaki, J. C. Hicks, A. Rousseau, F. Thevenet, A. Khacef and M. Carreon, *J. Phys. D: Appl. Phys.*, 2020, **53**, 1–51.
9 K. H. R. Rouwenhorst, F. Jardali, A. Bogaerts and L. Lefferts, *Energy Environ. Sci.*, 2023, **16**, 6170–6173.
10 A. Bogaerts and E. C. Neyts, *ACS Energy Lett.*, 2018, **3**, 1013–1027.
11 E. Vervloessem, Y. Gorbanev, A. Nikiforov, N. De Geyter and A. Bogaerts, *Green Chem.*, 2022, **24**, 916–929.
12 W. A. Dekker, E. Snoeck and H. Kramers, *Chem. Eng. Sci.*, 1959, **11**, 61–71.
13 X. Pei, D. Gidon, Y. J. Yang, Z. Xiong and D. B. Graves, *Chem. Eng. J.*, 2019, **362**, 217–228.
14 U. Kogelschatz, *Plasma Chem. Plasma Process.*, 2003, **23**, 1–46.

530 | *React. Chem. Eng.*, 2024, **9**, 528–531

This journal is © The Royal Society of Chemistry 2024

15 B. S. Patil, N. Cherkasov, J. Lang, A. O. Ibhadon, V. Hessel and Q. Wang, *Appl. Catal., B*, 2016, **194**, 123–133.

16 Q. Sun, A. Zhu, X. Yang, J. Niu and Y. Xu, *Chem. Commun.*, 2003, 1418–1419.

17 A. A. Abdelaziz and H.-H. Kim, *J. Phys. D: Appl. Phys.*, 2020, **53**, 114001–114018.

18 Y. Ma, Y. Wang, J. Harding and X. Tu, *Plasma Sources Sci. Technol.*, 2021, **30**, 105002–105013.

19 K. H. R. Rouwenhorst, S. Mani and L. Lefferts, *ACS Sustainable Chem. Eng.*, 2022, **10**, 1994–2000.

20 C. Verrier, J. H. Kwak, D. H. Kim, C. H. F. Peden and J. Szanyi, *Catal. Today*, 2008, **136**, 121–127.

21 T. H. Y. Duong, T. N. Nguyen, H. T. Oanh, T. A. Dang Thi, L. N. T. Giang, H. T. Phuong, N. T. Anh, B. M. Nguyen, V. T. Quang, G. T. Le and T. Van Nguyen, *J. Chem.*, 2019, **2019**, DOI: **10.1155/2019/4376429**.

22 K. H. R. Rouwenhorst and L. Lefferts, *Catalysts*, 2020, **10**(9), DOI: **10.3390/catal10090999**.

23 A. ul R. Salman, B. C. Enger, X. Auvray, R. Lødeng, M. Menon, D. Waller and M. Rønning, *Appl. Catal., A*, 2018, **564**, 142–146.

24 H.-H. Kim, Y. Teramoto, A. Ogata, H. Takagi and T. Nanba, *Plasma Processes Polym.*, 2017, **14**, 1–9.

25 P. Peng, P. Chen, M. Addy, Y. Cheng, E. Anderson, N. Zhou, C. Schiappacasse, Y. Zhang, D. Chen, R. Hatzenbeller and Y. Liu, *ACS Sustainable Chem. Eng.*, 2019, 7, 100–104.

26 K. H. R. Rouwenhorst and L. Lefferts, *Plasma Processes Polym.*, 2023, 1–8.

This journal is © The Royal Society of Chemistry 2024

React. Chem. Eng., 2024, **9**, 528–531 | **531**